On the Polyphase Decomposition for Design of Generalized Comb Decimation Filters

Massimiliano Laddomada, *Member, IEEE*

***Abstract*—Generalized comb filters (GCFs) are efficient anti-aliasing decimation filters with improved selectivity and quantization noise (QN) rejection performance around the so called folding bands with respect to classical comb filters. In this paper, we address the design of GCF filters by proposing an efficient partial polyphase architecture with the aim to reduce the data rate as much as possible after the ΣΔ A/D conversion. We propose a mathematical framework in order to completely characterize the dependence of the frequency response of GCFs on the quantization of the multipliers embedded in the proposed filter architecture. This analysis paves the way to the design of multiplier-less decimation architectures. We also derive the impulse response of a sample third-order GCF filter used as reference scheme throughout the paper.**

***Index Terms*—CIC-filters, comb, decimation, decimation filter, delta, delta-sigma, generalized comb filter (GCF), partial polyphase, polyphase, power-of-2, sigma, sigma-delta, sinc filters, ΣΔ.**

I. Introduction and Problem Formulation

THE design of computationally efficient decimation filters for ΣΔ analog–digital (A/D) converters is a well-known research topic [1]–[3]. Given a base-band analog input signal $x(t)$ with bandwidth $[-f_x, +f_x]$, a ΣΔ A/D converter of order B produces a digital signal $x(nT_s)$ by sampling $x(t)$ at rate $f_s = 2\rho f_x \gg 2f_x$, whereby ρ is the so-called oversampling ratio. The normalized maximum frequency contained in the input signal is defined as $f_c = f_x/f_s = 1/2\rho$, and the digital signal $x(nT_s)$ at the input of the first decimation filter has frequency components belonging to the range $f_d \in [-f_c, f_c]$ (where f_d denotes the digital frequency). This setup is pictorially depicted in the reference architecture shown in Fig. 1.

Owing to the condition $\rho \gg 1$, the decimation of an oversampled signal $x(nT_s)$ is efficiently [4] accomplished by cascading two (or more) decimation stages, as highlighted in Fig. 1, followed by a finite-impulse response (FIR) filter that provides the required selectivity on the sampled signal $x(nT_N)$ at baseband. The first decimation filter is usually an Nth-order comb filter decimating by D [2], [3], [5], whereby the order N has to be greater or equal to $B+1$ [1], [3].

The design of a multistage decimation filter for ΣΔ converters poses stringent constraints on the shape of the frequency response of the first decimation stage. Considering the scheme in Fig. 1, the frequency response $H_1(e^{j\omega})$ of the first decimation filter must attenuate the quantization noise (QN) falling inside the so called folding bands, i.e., the frequency ranges defined as $[(k/D) - f_c; (k/D) + f_c]$ with $k = 1, \ldots, \lfloor D/2 \rfloor$ if D is even, and $k = 1, \ldots, \lfloor (D-1)/2 \rfloor$ for D odd (for conciseness, the set of values assumed by k will be denoted as K_k throughout the paper). The reason is that the ΣΔ QN falling inside these frequency bands, will fold down to baseband because of the sampling rate reduction by D in the first decimation stage, inevitably affecting the signal resolution after the multistage decimation chain. This issue is especially important for the first decimation stage, since the QN folding down to baseband has not been previously attenuated. Fig. 1 also shows the frequency range $[0, f_c]$ where the useful signal bandwidth falls, along with the so called *don't care* bands, i.e., the frequency ranges whose QN will be rejected by the filters placed beyond the first decimation stage.

In connection with the first decimation stage in the multistage architecture shown in Fig. 1, the required aliasing protection around the folding bands is usually guaranteed by a comb filter, which provides an inherent antialising function by placing its zeros in the middle of each folding band. We recall that the transfer function of a Nth-order comb filter is defined as [2]

$$H_{C_N}(z) = \left(\frac{1}{D}\frac{1-z^{-D}}{1-z^{-1}}\right)^N = \frac{1}{D^N}\prod_{i=1}^{D-1}\left(1 - z^{-1}e^{j\frac{2\pi}{D}i}\right)^N \tag{1}$$

where D is the desired decimation factor.

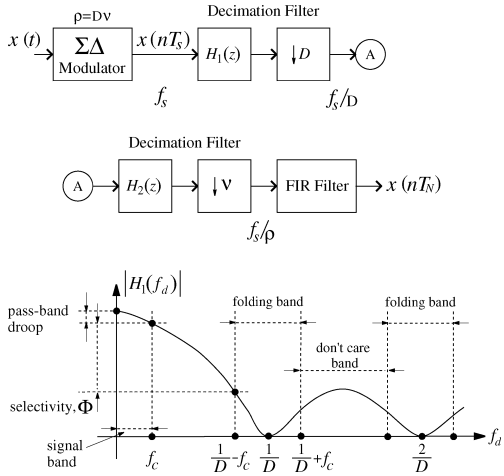

Fig. 1. General architecture of a two-stage decimation chain for ΣΔ A/D converters, along with a pictorial representation of the key frequency intervals to be carefully considered for the design of the first decimation stage.

Manuscript received February 6, 2007; revised August 14, 2007, and December 6, 2007. First published March 7, 2008; current version published September 17, 2008. This paper was recommended by Associate Editor A. Kummert.

The author is with the Electrical Engineering Department, Texas A&M University, Texarkana, TX 75505 USA (e-mail: mladdomada@tamut.edu).

Digital Object Identifier 10.1109/TCSI.2008.920136

With this background, let us provide a quick survey of the recent literature related to the problem addressed here. This survey is by no means exhaustive and is meant to simply provide a sampling of the literature in this fertile area.

A third-order modified decimation sinc filter was proposed in [6], and still further analyzed in [7], [8]. The class of comb filters was then generalized in [9], whereby the authors proposed an optimization framework for deriving the optimal zero rotations of generalized comb filters (GCFs) for any filter order and decimation factor D.

Other works somewhat related to the topic addressed in this paper are [10]–[16]. In [10] and [11] authors proposed computational efficient decimation filter architectures for implementing classical comb filters. In [12] authors proposed the use of decimation sharpened filters embedding comb filters, whereas in [13] authors addressed the design of a novel two-stage sharpened comb decimator. In [14], [15], authors proposed novel decimation schemes for $\Sigma\Delta$ A/D converters based on Kaiser and Hamming sharpened filters, then generalized in [16] for higher order decimation filters.

The main aim of this paper is to propose a flexible, yet effective, partial polyphase architecture for implementing the GCF filters proposed in the companion paper [9]. To this end, we first recall the z-transfer function of GCF filters for completeness, and, then, provide a mathematical formulation for deriving the impulse response of this class of decimation filters. The latter is needed for deriving the polyphase components of the proposed filters. In the second part of the paper, the focus is on the sensitivity of the frequency response of GCF filters due to the quantization of the multipliers embedded in the proposed architecture. We also analyze zero displacements in the z-transfer function of GCF filters for deducing useful hints at the basis of any practical implementation of such filters.

The rest of the paper is organized as follows. In Section II, we briefly recall the transfer functions of GCF filters and highlight their main peculiarities with respect to classical comb filters. Section III presents an effective architecture, namely a partial polyphase decomposition, for implementing GCF decimation filters; the impulse response of a sample third-order GCF filter is also presented, and mathematically derived in the Appendix. In Section IV, we present a mathematical framework for evaluating the sensitivity of the frequency response of GCF filters to the approximations of the embedded multipliers. Zero displacements due to multiplier approximation is discussed in Section V, where we also draw general guidelines for the design of such filters. Finally, Section VI draws the conclusions.

II. The z-Transfer Function of GCF Filters

In this section, we briefly recall the z-transfer function of GCF filters proposed in [9]. The z-transfer function $H_{\mathrm{GCF}_N}(z)$ of a Nth-order GCF filter decimating by D is defined as

$$\begin{cases} \frac{1}{H_{o,ev,1}} H_1(z) \cdot \prod_{n=1}^{\lfloor \frac{N}{2} \rfloor} H_2(z, \alpha_{n+N}), & D \text{ even},\ N \text{ even} \\ \frac{(1+z^{-1})}{H_{o,ev,2}} H_1(z) \cdot \prod_{n=1}^{\lfloor \frac{N}{2} \rfloor} H_2(z, \alpha_{n+N}), & D \text{ even},\ N \text{ odd} \\ \frac{1}{H_{o,od}} H_1(z), & D \text{ odd} \end{cases} \tag{2}$$

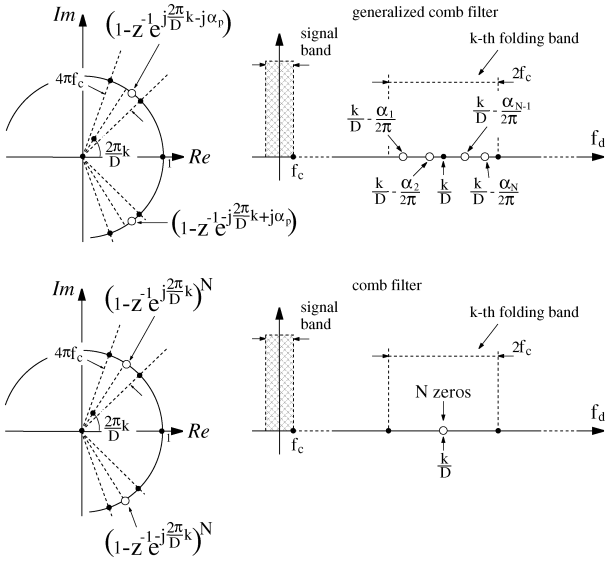

Fig. 2. Zero locations of the considered decimation filters within the kth folding band. Zeros are displayed in the z-plane and in the frequency axis in order to highlight their effect in both domains.

whereby the involved basic functions are defined as follows:

$$\begin{aligned} H_1(z) &= \prod_{i=1}^{D_M} \prod_{n=1}^{N} \left(1 - 2\cos\left(\frac{2\pi}{D} i - \alpha_n\right) z^{-1} + z^{-2}\right) \\ &= \prod_{i=1}^{D_M} \prod_{n=1}^{N} \left(1 - z^{-1} e^{+j\frac{2\pi}{D} i - j\alpha_n}\right) \\ &\quad \times \left(1 - z^{-1} e^{-j\frac{2\pi}{D} i + j\alpha_n}\right) \end{aligned} \tag{3}$$

with $D_M = (D/2) - 1$, for D even, and $D_M = (D-1)/2$, for D odd, and

$$H_2(z, \alpha_{n+N}) = 1 - 2\cos(\pi - \alpha_{n+N}) z^{-1} + z^{-2}. \tag{4}$$

Terms $H_{o,ev,1}$, $H_{o,ev,2}$, and $H_{o,od}$ are appropriate normalization constants chosen in such a way as to have $H_{\mathrm{GCF}_N}(z)|_{z=1} = 1$, and $\lfloor \cdot \rfloor$ is the floor of the underlined number.

Let us summarize the main peculiarities of GCF filters by comparing them to classical comb filters. GCFs are, as comb filters, linear-phase filters since they are constituted by two linear-phase basic filters, namely $H_1(z)$ and $H_2(z)$.

An Nth-order comb filter (1) decimating by D, places Nth-order zeros in the complex locations $z_i = e^{j(2\pi/D)i}$, $\forall i = 1, \ldots, D-1$, or, equivalently, in the digital frequencies $f_{z_k} = k/D$, $k \in K_k$. On the other hand, an Nth-order GCF filter decimating by D places N pairs of conjugate complex zeros in the ith folding band[1], with $i = 1, \ldots, D_M$, as exemplified by the function $H_1(z)$ in (2). A pictorial representation of the zero locations of a GCF filter is given in Fig. 2. The behavior of the function $H_2(z)$ is analogous to that of $H_1(z)$ with the exception that its zeros are placed around the location $z = -1$ in the z-complex plane, and, it holds only for D even. A convenient choice for α_p is $\alpha_p = q_p 2\pi f_c$, with $q_p \in [-1, +1]$: this solution is such that each pair of conjugate complex zeros

[1]For conciseness, we only deal with the positive semi-plane in the z-domain; however, the zero placement is specular for what concerns the zeros located in the lower semi-plane.

TABLE I
OPTIMAL PARAMETERS OF GCF DECIMATION FILTERS

N	3	4	5	6
q_1	-0.79	-0.35	+0.55	+0.95
q_2	0.0	+0.35	+0.93	+0.675
q_3	+0.79	-0.88	-0.55	+0.25
q_4	+0.79	+0.88	-0.93	-0.25
q_5	-	+0.88	0.0	-0.675
q_6	-	+0.35	+0.55	-0.95
q_7	-	-	+0.93	+0.95
q_8	-	-	-	+0.675
q_9	-	-	-	+0.25
$G-[dB]$	$\sim$8	$\sim$13	$\sim$18	$\sim$ 23

falls inside the relative folding band guaranteeing the required selectivity in these frequency bands. By virtue of the zero distribution within the folding bands, GCF filters provide improved $\Sigma\Delta$ QN rejection capabilities with respect to classical comb filters of the same order. For completeness, Table I shows the optimal zero rotations q_p found in [9] by minimizing the $\Sigma\Delta$ QN around the folding bands. As an example, a third-order GCF filter provides a $\Sigma\Delta$ QN rejection 8 dB higher than that guaranteed by a classical third-order comb filter. Throughout the paper, we will use this optimal choice of the zero rotations where no otherwise specified. We invite the interested readers to refer to [9] for further details about the characteristics along with the performance of GCF filters.

III. PARTIAL POLYPHASE DECOMPOSITION OF GCF FILTERS

This section presents a nonrecursive, partial polyphase implementation of GCF filters, suitable for decimation factors D that can be expressed as the pth power-of-two, i.e., $D = 2^p$ with p a suitable integer greater than zero. For conciseness, we only address the implementation of a third-order GCF filter, but the considerations that follow, can be easily extended to higher order GCF filters with D as specified above.

Let us focus on the optimal zero rotations shown in Table I, and consider the z-transfer function $H_{\mathrm{GCF}_3}(z)$ derived in (2). Due to the symmetry of q_p in Table I, the zeros belonging to $H_{\mathrm{GCF}_3}(z)$ can be collected in the following three z-transfer functions:

$$\prod_{i=1}^{D-1}\left(1-z^{-1}e^{j\frac{2\pi}{D}i}\right)=\frac{1-z^{-D}}{1-z^{-1}}$$
$$\prod_{i=1}^{D-1}\left(1-z^{-1}e^{j\frac{2\pi}{D}i}e^{-j\alpha}\right)=\prod_{i=1}^{D-1}\left(1-\beta_1^{-1}e^{j\frac{2\pi}{D}i}\right)$$
$$\prod_{i=1}^{D-1}\left(1-z^{-1}e^{j\frac{2\pi}{D}i}e^{+j\alpha}\right)=\prod_{i=1}^{D-1}\left(1-\beta_2^{-1}e^{j\frac{2\pi}{D}i}\right)$$

whereby $\beta_1 = z\cdot e^{j\alpha}$, $\beta_2 = z\cdot e^{-j\alpha}$, and $\alpha = |q_1|2\pi f_c$. Notice that the first z-transfer function accounts for the zeros falling in the digital frequencies k/D, $k \in K_k$, which correspond to the zeros of a classical first-order comb filter. The other two z-transfer functions consider the rotated zeros.

The z-transfer function $H_{\mathrm{GCF}_3}(z)$ can be easily obtained by multiplying the previous three z-transfer functions[2]

$$H_{\mathrm{GCF}_3}(z)=\frac{1-z^{-D}}{1-z^{-1}}\frac{1-z^{-D}e^{j\alpha D}}{1-z^{-1}e^{j\alpha}}\frac{1-z^{-D}e^{-j\alpha D}}{1-z^{-1}e^{-j\alpha}}. \quad (5)$$

The impulse response of the third-order GCF filter in (5) has been derived in the Appendix.

A nonrecursive implementation of filter $H_{\mathrm{GCF}_3}(z)$ can be obtained by expressing each rational function in (5) in non recursive form. By doing so, the first polynomial ratio can be rewritten as follows:

$$\frac{1-z^{-D}}{1-z^{-1}}=\sum_{i=0}^{D-1}z^{-i}=\prod_{i=0}^{\log_2(D)-1}\left(1+z^{-2^i}\right) \quad (6)$$

whereby last equality holds for $D = 2^p$. Upon using a similar reasoning, it is straightforward to observe that the following equality chain, which derives from (6) by imposing $\beta = z\cdot e^{\mp j\alpha}$, holds as well

$$\frac{1-z^{-D}e^{\pm j\alpha D}}{1-z^{-1}e^{\pm j\alpha}}=\sum_{i=0}^{D-1}z^{-i}e^{\pm ji\alpha}=\prod_{i=0}^{\log_2(D)-1}\left(1+z^{-2^i}e^{\pm j2^i\alpha}\right). \quad (7)$$

By noting that

$$\left(1+z^{-2^i}e^{+j2^i\alpha}\right)\left(1+z^{-2^i}e^{-j2^i\alpha}\right)=1+2\cos(2^i\alpha)z^{-2^i}+z^{-2^{i+1}}$$

after some algebra, (5) can be rewritten as follows:

$$\begin{aligned}H_{\mathrm{GCF}_3}(z)&=\prod_{i=0}^{\log_2(D)-1}\left[\left(1+z^{-2^i}\right)\cdot\left(1+2\cos(2^i\alpha)z^{-2^i}+z^{-2^{i+1}}\right)\right]\\&=\prod_{i=0}^{\log_2(D)-1}\left[1+r_i\cdot\left(z^{-2^i}+z^{-2\cdot 2^i}\right)+z^{-3\cdot 2^i}\right]\end{aligned} \quad (8)$$

whereby

$$\begin{aligned}r_i&=1+2\cos(2^i\alpha)=1+2\cos\left(q\frac{2^i\pi}{\rho}\right)\\&=1+2\cos(q2^{i+1}\pi f_c),\ \forall i=0,\ldots,\log_2(D)-1.\end{aligned}$$

Assume that the decimation factor D can be decomposed as follows $D = D_1\cdot D_2$, whereby $D_1 = 2^{p_p+1}$ and $D_2 = 2^{p-p_p-1}$. By doing so, (8) can be rewritten as follows:

$$H_{\mathrm{GCF}_3}(z)=H_P(z)\cdot H_N(z) \quad (9)$$

[2]Notice that, for conciseness, in the mathematical formulation that follows, we omit the constant term assuring unity gain at base-band.

whereby

$$H_P(z) = \prod_{i=0}^{p_p} \left[1+r_i \cdot \left(z^{-2^i}+z^{-2\cdot 2^i}\right)+z^{-3\cdot 2^i}\right]$$

$$H_N(z) = \prod_{i=p_p+1}^{p-1} \left[1+r_i \cdot \left(z^{-2^i}+z^{-2\cdot 2^i}\right)+z^{-3\cdot 2^i}\right] \quad (10)$$

Remembering that $p_p = \log_2(D_1) - 1$, it is straightforward to observe that $H_P(z)$ is the z-transfer function of a third-order GCF filter decimating by D_1. The impulse response $h_P(n)$, $\forall n \in [0, 3D_1-3]$, of filter $H_P(z)$ has been derived in Appendix

$$h_P(n) = e^{+j\alpha n} \sum_{k_3=0}^{n} e^{-2j\alpha k_3} \sum_{k_2=0}^{k_3} e^{j\alpha k_2} \sum_{k_1=0}^{k_2} x_t(k_1). \quad (11)$$

The sequence $x_t(n)$ is defined as follows:

$$x_t(n) = \delta(n)-r\delta(n-D_1)+r\delta(n-2D_1)-\delta(n-3D_1) \quad (12)$$

whereby $r = 1 + \cos(\alpha D_1)$, and $\alpha = |q_1|\pi(1/\rho)$.

The polyphase decomposition of the z-transfer function $H_P(z)$ is defined as follows:

$$H_P(z) = \sum_{k=0}^{D_1-1} z^{-k} E_k(z^{D_1}) \quad (13)$$

whereby the functions $E_k(z)$ are the polyphase components. Time-domain coefficients related to $E_k(z)$ are defined as follows:

$$e_k(n) = h_P(D_1 n + k), \ \forall k \in [0, D_1 - 1] \quad (14)$$

and can be easily obtained by employing the recursive equation in (11).

Some observations are in order. By choosing $p_p = p-1$, GCF filter $H_{\mathrm{GCF}_3}(z)$ is fully realized in polyphase form, whereas for $p_p = -1$ the overall decimator is realized as the cascade of p non recursive decimation stages each one decimating by 2. Any other value of $p_p \in [0, p-2]$ yields a partial polyphase decomposition.

The natural question that arises at this point concerns the practical implementation of the GCF filter $H_{\mathrm{GCF}_3}(z)$. In the following we derive an architecture for implementing GCF filters, while in the next section we present a mathematical framework for highlighting the sensitivity of the proposed architecture to the approximation of its multipliers. The latter is needed for deducing useful hints at the basis of multiplier-less implementations of the proposed filters.

By applying the commutative property employed in [5], it is possible to obtain the cascaded architecture shown in Fig. 3. The first polyphase decimation stage allows the reduction of the sampling rate by D_1, thus reducing the operating rate of the subsequent decimation stages belonging to $H_N(z)$. Any stage of $H_N(z)$ in Fig. 3 is constituted by a simple FIR filter operating at a different rate. Such an example, the ith stage, with $i \in [0, p-p_p-2]$, is characterized by the transfer function $[1 + r_i(z^{-1}+z^{-2})+z^{-3}]$ operating at rate $f_s/(D_1 \cdot 2^i)$ (f_s is the $\Sigma\Delta$ sampling frequency).

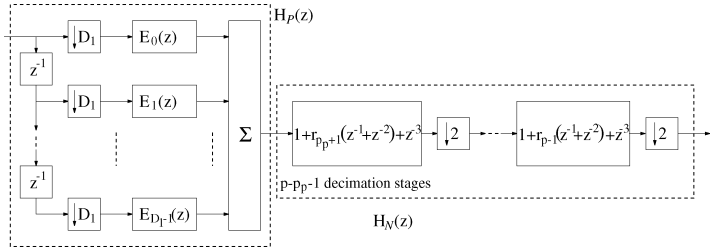

Fig. 3. Architecture of the partial polyphase implementation of the decimation filter $H_{\mathrm{GCF}_3}(z)$. The overall decimation factor $D = D_1 \cdot D_2$ is split between the polyphase section decimating by $D_1 = 2^{p_p+1}$, and the non recursive section, decimating by $D_2 = 2^{p-p_p-1}$, composed of $p-p_p-1$ decimation stages each one decimating by 2. Integer p_p can take on any value in the set $[-1, p-1]$.

The frequency response related to $H_N(z)$ can be evaluated by substituting $z = e^{j\omega}$ in (10)

$$H_N(e^{j\omega}) = 2 \prod_{u=p_p+1}^{p-1} e^{-j3\cdot 2^{u-1}\omega} \cdot \left[\cos(3 \cdot 2^{u-1}\omega) + r_u \cos(2^{u-1}\omega)\right] \quad (15)$$

whereby $\omega = 2\pi f_d$, and r_u is defined as

$$r_u = 1 + 2\cos(2^u \alpha), \ \forall u = p_p + 1, \ldots, p-1. \quad (16)$$

IV. Sensitivity Analysis

This section deals with the analysis of the sensitivity of filter $H_{\mathrm{GCF}_3}(z)$ to the approximation of its multipliers. In brief, the goal is to design the nonrecursive architecture in Fig. 3 without multipliers, while guaranteeing the gain (8 dB based on the results shown in Table I) in terms of $\Sigma\Delta$ QN rejection with respect to a classical comb filter.

Let us evaluate the sensitivity of the frequency response in (9) with respect to its coefficients. Notice that there are two sets of coefficients: $L = 3D_1 - 2$ multipliers (i.e., $c_{n,k} = h_P(D_1 n + k)$) belong to the polyphase section $H_P(z)$, and $p - p_p - 1$ multipliers r_u [shown in (16)] belong to the decimation filter $H_N(z)$.

First of all, notice that when the generic coefficient $c_{n,k}$ (r_u) is approximated, its actual value can be expressed as $\widetilde{c}_{n,k} = c_{n,k} + \Delta c_{n,k} (\widetilde{r}_u = r_u + \Delta r_u)$, whereby $\Delta c_{n,k} (\Delta r_u)$ is the approximation error. On the other hand, the approximations of coefficients $c_{n,k}$ and r_u imply that $H_{\mathrm{GCF}_3}(e^{j\omega})$ be written as

$$\widetilde{H}_{\mathrm{GCF}_3}(e^{j\omega}) = H_{\mathrm{GCF}_3}(e^{j\omega}) + \Delta H_{\mathrm{GCF}_3}(e^{j\omega}) \quad (17)$$

The dependence of the frequency response $H_{\mathrm{GCF}_3}(e^{j\omega})$ on the approximation of its multipliers can be evaluated by differentiating (9)

$$\Delta H_{\mathrm{GCF}_3}(e^{j\omega}) = H_N(e^{j\omega})\Delta H_P(e^{j\omega}) + H_P(e^{j\omega})\Delta H_N(e^{j\omega}) \quad (18)$$

whereby

$$H_P(e^{j\omega})\Delta H_N(e^{j\omega}) = H_P(e^{j\omega}) \sum_{u=p_p+1}^{p-1} \frac{\partial H_N(e^{j\omega})}{\partial r_u} \Delta r_u \quad (19)$$

and

$$H_N(e^{j\omega})\Delta H_P(e^{j\omega}) = H_N(e^{j\omega})\left[\sum_{k,n}\frac{\partial H_P(e^{j\omega})}{\partial c_{n,k}}\Delta c_{n,k}\right] \tag{20}$$

with

$$H_P(e^{j\omega}) = \sum_{k=0}^{D_1-1}\sum_{n=0}^{\lfloor L/D_1\rfloor} c_{n,k}e^{-j\omega(D_1n+k)}. \tag{21}$$

Let us evaluate the derivative of $H_N(e^{j\omega})$ with respect to r_u, $\forall u = p_p+1,\ldots,p-1$

$$\frac{\partial H_N(e^{j\omega})}{\partial r_u} = 2e^{-j3\cdot 2^{u-1}\omega}\cos(2^{u-1}\omega)\prod_{m=p_p+1,m\neq u}^{p-1} e^{-j3\cdot 2^{m-1}\omega} \times\left[\cos(3\cdot 2^{m-1}\omega)+r_m\cdot\cos(2^{m-1}\omega)\right]. \tag{22}$$

Equation (22) can be rewritten as follows:

$$\frac{\partial H_N(e^{j\omega})}{\partial r_u} = H_N(e^{j\omega})\cdot\frac{\cos(2^{u-1}\omega)}{\cos(3\cdot 2^{u-1}\omega)+r_u\cdot\cos(2^{u-1}\omega)} \tag{23}$$

Upon substituting (23) in (19), it is possible to obtain

$$\begin{aligned} H_P(e^{j\omega})&\Delta H_N(e^{j\omega}) \\ &= H_P(e^{j\omega})H_N(e^{j\omega}) \\ &\quad\cdot\sum_{u=p_p+1}^{p-1}\frac{\cos(2^{u-1}\omega)\Delta r_u}{\cos(3\cdot 2^{u-1}\omega)+r_u\cdot\cos(2^{u-1}\omega)} \\ &= H_{\mathrm{GCF}_3}(e^{j\omega}) \\ &\quad\cdot\sum_{u=p_p+1}^{p-1}\frac{\cos(2^{u-1}\omega)\Delta r_u}{\cos(3\cdot 2^{u-1}\omega)+r_u\cdot\cos(2^{u-1}\omega)}. \end{aligned} \tag{24}$$

Let us consider $\Delta H_P(e^{j\omega})$. Given $H_P(e^{j\omega})$ in (21), it is straightforward to obtain the following relation:

$$\frac{\partial H_P(e^{j\omega})}{\partial c_{n,k}} = e^{-j\omega(D_1n+k)}.$$

By substituting the previous equation in (20), it is possible to obtain

$$\Delta H_P(e^{j\omega}) = \sum_{k=0}^{D_1-1}\sum_{n=0}^{\lfloor L/D_1\rfloor}\Delta c_{n,k}e^{-j\omega(D_1n+k)}.$$

Upon multiplying and dividing by $H_P(e^{j\omega})$, the function $H_N(e^{j\omega})\Delta H_P(e^{j\omega})$ can be rewritten as

$$\frac{H_{\mathrm{GCF}_3}(e^{j\omega})}{H_P(e^{j\omega})}\sum_{k=0}^{D_1-1}\sum_{n=0}^{\lfloor L/D_1\rfloor}\Delta c_{n,k}e^{-j\omega(D_1n+k)}. \tag{25}$$

The actual frequency response $\widetilde{H}_{\mathrm{GCF}_3}(e^{j\omega})$ in (17) can be expressed as follows:

$$\begin{aligned} &\widetilde{H}_{\mathrm{GCF}_3}(e^{j\omega}) \\ &\quad= H_{\mathrm{GCF}_3}(e^{j\omega}) + \Delta H_{\mathrm{GCF}_3}(e^{j\omega}) \\ &\quad= H_{\mathrm{GCF}_3}(e^{j\omega}) \\ &\qquad\cdot\left[1+\frac{1}{H_P(e^{j\omega})}\sum_{k=0}^{D_1-1}\sum_{n=0}^{\lfloor L/D_1\rfloor}\left[\Delta c_{n,k}\cdot e^{-j\omega(D_1n+k)}\right]\right. \\ &\qquad\left.+\sum_{i=p_p+1}^{p-1}\frac{\cos(2^{i-1}\omega)\Delta r_i}{\cos(3\cdot 2^{i-1}\omega)+r_i\cdot\cos(2^{i-1}\omega)}\right]. \end{aligned} \tag{26}$$

The effects of the approximation of the multipliers $c_{n,k}$ and r_u on the actual frequency response $\widetilde{H}_{\mathrm{GCF}_3}(e^{j\omega})$ can be understood by analyzing the frequency behavior of the following error function:

$$\begin{aligned} \Delta H(e^{j\omega}) &= \frac{1}{H_P(e^{j\omega})}\sum_{k=0}^{D_1-1}\sum_{n=0}^{\lfloor L/D_1\rfloor}\left[\Delta c_{n,k}\cdot e^{-j\omega(D_1n+k)}\right] \\ &\quad+\sum_{i=p_p+1}^{p-1}\frac{\cos(2^{i-1}\omega)\Delta r_i}{\cos(3\cdot 2^{i-1}\omega)+r_i\cdot\cos(2^{i-1}\omega)} \\ &= \Delta H_1(e^{j\omega})+\sum_{i=p_p+1}^{p-1}\Delta H_{2,i}(e^{j\omega}) \end{aligned} \tag{27}$$

which, to some extent, quantifies the distortion between the desired $H_{\mathrm{GCF}_3}(e^{j\omega})$ and the actual frequency response $\widetilde{H}_{\mathrm{GCF}_3}(e^{j\omega})$.

Let us derive some observations from the sensitivity analysis above. To this end, in what follows we adopt the design parameters summarized in Table II.

Fig. 4 depicts the frequency behaviors of the error functions $\Delta H_1(e^{j\omega})$ and $\Delta H_{2,i}(e^{j\omega})$ noted in the last row of (27), for the following sample set of parameters: $D = 32$, $D_1 = 8$, $D_2 = 4$, $p_p = 2$, $p = 5$, $\nu = 4$, $q = |q_1| = 0.79$, and $\Delta h_P(n) = \Delta r_i = 10^{-4}$, $\forall n, i$ (see also Table II).

Fig. 5 shows the behaviors of the frequency responses $H_P(e^{j\omega})$ and $H_N(e^{j\omega})$ for the sample set of parameters summarized in Table II. For comparisons, in both subplots we also show the frequency response (dashed curve) of a classical third-order comb filter in (1), along with the extents of the folding bands[3], pictorially depicted with vertical lines centered around the frequencies

$$\frac{k}{D}\pm f_c = \frac{k}{32}\pm 3.9\cdot 10^{-3}, \qquad k = 1,\ldots,16. \tag{28}$$

Finally, Fig. 6 compares the frequency behaviors (in decibels) of the frequency responses of $H_{\mathrm{GCF}_3}(e^{j\omega})$ and $H_{C_3}(e^{j\omega})$ (classical third-order comb filter in (1)) along the whole frequency range [0, 1/2] (upper subplot) and within the first folding band $[1/32-f_c; 1/32+f_c]$ (lower subplot). The figure also identifies the folding bands noted in (28).

[3]Notice that such folding bands also apply to the subplots shown in Fig. 4.

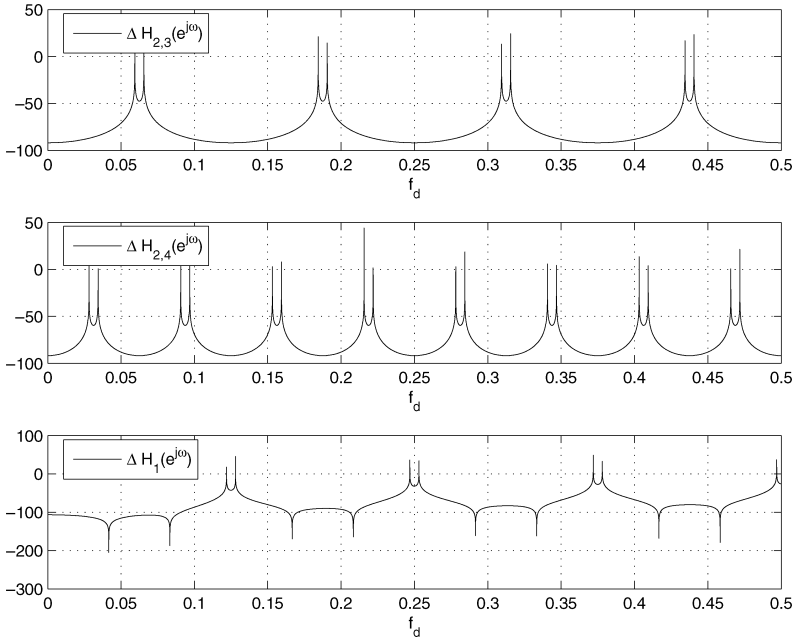

Fig. 4. Frequency behaviors in decibels of the functions $|\Delta H_1(e^{j\omega})|$, $|\Delta H_{2,3}(e^{j\omega})|$, and $|\Delta H_{2,4}(e^{j\omega})|$ in (27) for $D_1 = 8$, $D_2 = 4$, $\nu = 4$, $q = 0.79$, and $\Delta h_P(n) = \Delta r_i = 10^{-4}$, $\forall n, i$.

TABLE II
DESIGN PARAMETERS EMPLOYED IN FIGS. 4, 5

$D = D_1 \cdot D_2 = 2^p = 32\big\vert_{p=5}$
Dec. factor of $H_{GCF_3}(e^{j\omega}) = H_P(e^{j\omega})H_N(e^{j\omega})$
$D_1 = 2^{p_p+1} = 2^3,\ p_p = 2$
Dec. factor of $H_P(e^{j\omega})$ (polyphase subfilter)
$D_2 = 2^{p-p_p-1} = 2^2,\ p_p = 2$
Dec. factor of $H_N(e^{j\omega})$. Integer $p - p_p - 1$ is the number of non recursive filters decimating by 2 in Fig. 3
$\nu = 4$, $\rho = D \cdot \nu = D_1 \cdot D_2 \cdot \nu = 128$, oversampling factor
$\alpha = 2\pi\vert q\vert f_c = 0.019\big\vert_{\vert q\vert=0.79}$, $f_c = \frac{1}{2\rho} = 3.9 \cdot 10^{-3}$

Some key observations are in order. Figs. 5 and 6 show that a classical third-order comb filter places its third-order zeros in the digital frequencies $k/D = k/32$, $k = 1, \ldots, 16$, while a third-order GCF filter distributes such zeroes within each folding band. Indeed, a third-order GCF filter with the parameters noted in Table II, is able to place its zeros in the digital frequencies k/D and $(k/D) \pm qf_c = (k/32) \pm q3.9 \cdot 10^{-3}$, $k = 1, \ldots, 16$. Since the optimal value q is less than one, three zeros fall within each folding band. This behavior is clearly highlighted in the lower subplot of Fig. 6, which shows the zeros of both $H_{\mathrm{GCF}_3}(e^{j\omega})$ and $H_{C_3}(e^{j\omega})$ around the first folding band.

Fig. 4 shows that the pass-band behavior of the filter $H_{\mathrm{GCF}_3}(e^{j\omega})$ is not affected by the approximation of its coefficients. Sensitivity of $H_{\mathrm{GCF}_3}(e^{j\omega})$ is very low for $f_d \in [0, f_c]$, whereby $f_c = 1/2\rho$. This in turn suggests that the filter pass-band droop does not degrade by virtue of multipliers' approximations, and it is as low as the one guaranteed by filter $H_{\mathrm{GCF}_3}(e^{j\omega})$. Notice also that the sensitivity is very low around the digital frequency $(1/D) - f_c$, which defines the selectivity of the decimation filter [1].

Figs. 4 and 5 show that the approximation of multipliers $h_P(n)$ and r_u affects the sensitivity of the frequency response $H_{\mathrm{GCF}_3}(e^{j\omega})$ in disjoint folding bands. Indeed, filters $H_P(e^{j\omega})$ and $H_N(e^{j\omega})$ place the respective zeros in different digital frequencies, as clearly highlighted in Fig. 5.

Fig. 4 shows that the frequency response $H_{\mathrm{GCF}_3}(e^{j\omega})$ is very sensitive to coefficients' approximations especially in the folding bands $[(k/D) - f_c, (k/D) + f_c]$, $k \in K_k$, since the peaks are centered in the zeros' frequencies $[(k/D) - 0.79 \cdot f_c, (k/D) + 0.79 \cdot f_c]$, $\forall k \in K_k$. This in turn suggests that particular care must be devoted to the approximation of multipliers embedded in both $H_P(z)$ and $H_N(z)$ in order to preserve the QN rejection performance around the folding bands. However, the same figure suggests that the approximation of the multipliers r_u belonging to $H_N(z)$, can be done independently from the approximations of coefficients $h_P(n)$ belonging to $H_P(z)$.

The analysis above was referred to a decimation factor $D = 32$ split as $D_1 = 2^3$ and $D_2 = 2^2$ between $H_P(e^{j\omega})$ and $H_N(e^{j\omega})$. For the sake of investigating the sensitivity of the proposed filters with respect to a different split between D_1 and D_2, Fig. 7 shows the frequency behaviors (in decibels) of the composite function $|\Delta H(e^{j\omega})|$ in (27) for three different combinations of D_1 and D_2 (as noted in the subplot titles), given the same overall decimation factor $D = D_1 \cdot D_2 = 2^5$. The other parameters are summarized in Table II. Leftmost subplot refers to the case $H_{\mathrm{GCF}_3}(e^{j\omega}) = H_N(e^{j\omega})$ (i.e., full cascaded implementation of the GCF filter) since $D_1 = 2^{p_p+1} = 1$ and $D_2 = D$, while the rightmost subplot refers to a full polyphase implementation (i.e., $H_{\mathrm{GCF}_3}(e^{j\omega}) = H_P(e^{j\omega})$) being $D_1 = D$ and $D_2 = 1$. Subplot in the middle refers to a partial polyphase implementation whereby $D_1 = 2^{p_p+1} = 2^3$ and $D_2 = 2^{p-p_p-1} = 2^2$; in connection to the architecture in Fig. 3, there are two non recursive stages decimating by 2 cascaded to the polyphase filter $H_P(e^{j\omega})$ decimating by 2^3. It is worth noticing that the sensitivity of $H_{\mathrm{GCF}_3}(e^{j\omega})$ tends

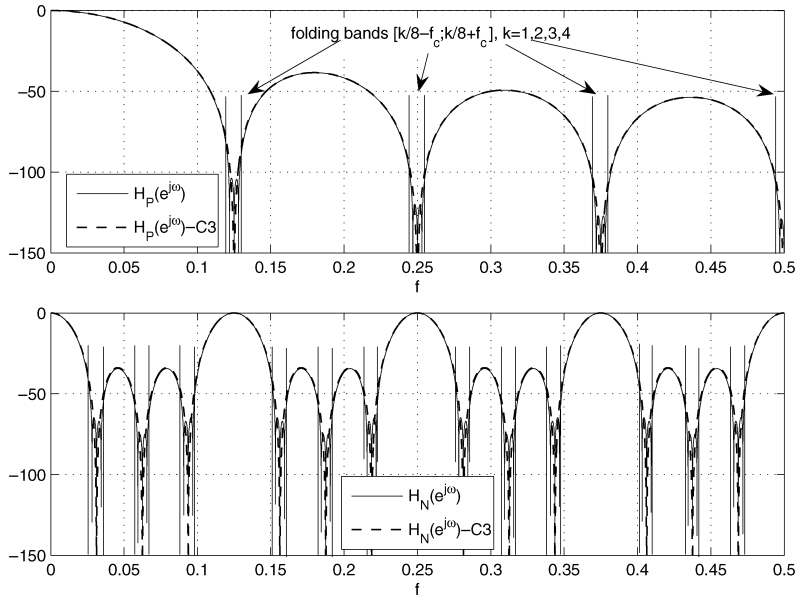

Fig. 5. Frequency behaviors in decibels of the functions $|H_P(e^{j\omega})|$ and $|H_N(e^{j\omega})|$, respectively, in (13) and (15) for $D_1 = 8$, $D_2 = 4$, $\nu = 4$, $q = 0.79$. The dashed curves in both subplots refer to the frequency response of a classical third-order comb filter.

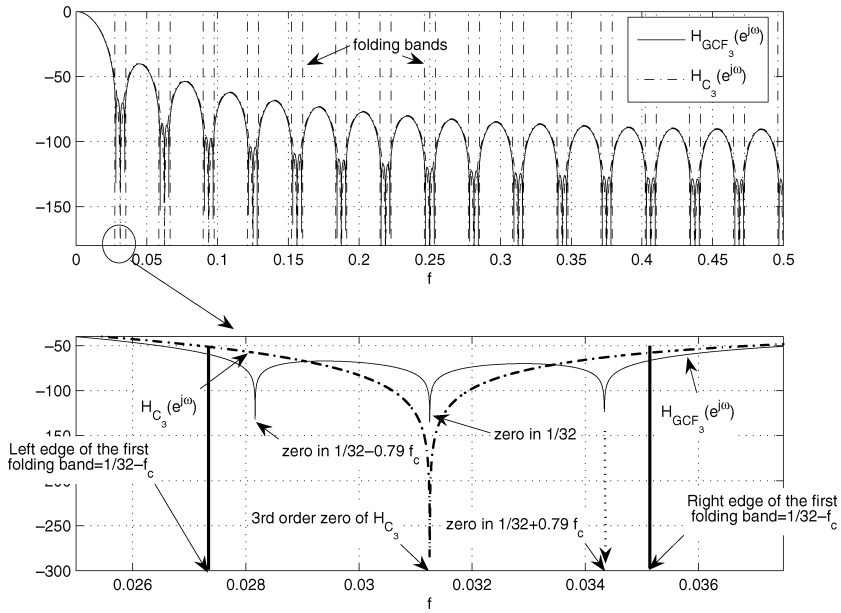

Fig. 6. The upper subplot shows the behaviors (in decibels) of the frequency responses $|H_{\mathrm{GCF}_3}(e^{j\omega})|$ and $|H_{C_3}(e^{j\omega})|$ (classical third-order comb filter in (1)) for $D = 2^5$, $\nu = 4$, and $q = 0.79$, while the lower subplot shows their behaviors around the first folding band $[1/32 - f_c; 1/32 + f_c]$. Vertical dashed-dot lines in the upper subplot identify the edge of the folding bands.

to decrease with the reduction of the number of non recursive stages decimating by 2 following the polyphase section. This is essentially due to the denominator in the summation appearing in (27), which tends to dominate the overall function $\Delta H(e^{j\omega})$. As a rule of thumb, it is preferable to reduce the number of non recursive stages belonging to $H_N(e^{j\omega})$ in order to contain the sensitivity of the overall filter $H_{\mathrm{GCF}_3}(e^{j\omega})$ to the approximation of its multipliers. On the other hand, given a decimation factor D, the choice of D_1 and D_2 can only be accomplished once an appropriate performance metric for the design at hand has been identified. In other words, higher values of D_1 correspond to longer impulse responses $h_P(n)$ (the filter length is $L = 3D_1 - 2$), which means higher area occupancy. However, higher values of D_1 can reduce the power consumption of the overall decimation filter, since the sampling data rate of the polyphase filters $E_0(z), \ldots, E_{D_1-1}(z)$ is f_s/D_1, whereby f_s is the $\Sigma\Delta$ sampling frequency. Therefore, depending on the specific requirements (area occupancy or power consumption) imposed to the decimation filter design, a value of D_1 as close as possible to D could be preferable. A final answer to this issue can only be given once a suitable performance metric cost function is specified.

Sensitivity analysis derived above, allows to draw a general picture of the effects of the approximations of the coefficients on

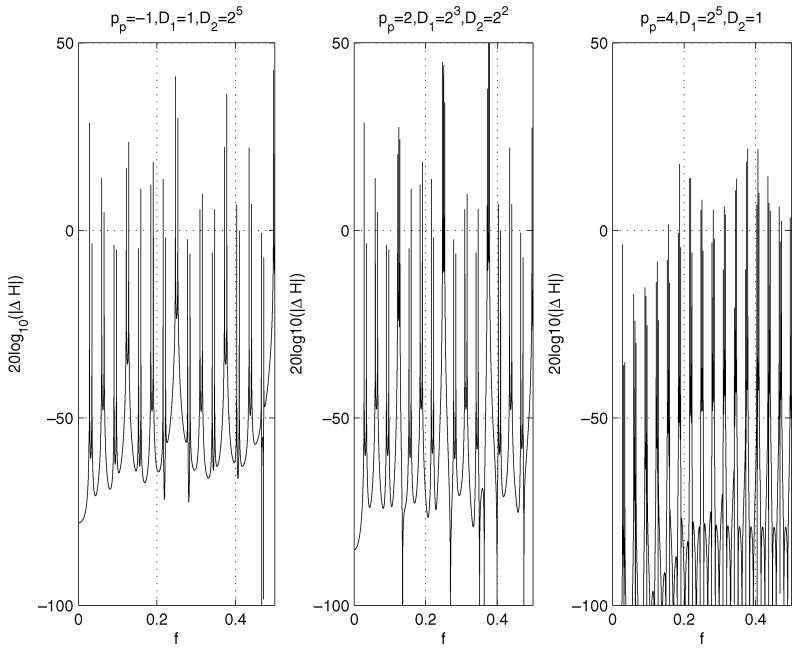

Fig. 7. Frequency behaviors in decibels of the functions $|\Delta H(e^{j\omega})|$ in (27), for $D = D_1 \cdot D_2 = 2^5$, $\nu = 4$, $q = 0.79$, and $\Delta h_P(n) = \Delta r_i = 10^{-4}$, $\forall n, i$, and for three different combinations of D_1 and D_2 as noted in the titles.

the actual frequency response $\widetilde{H}_{\mathrm{GCF}_3}(z)$. Nevertheless, we deduced that the sensitivity is very low in the pass-band $[0, f_c]$ and around the frequency $(1/D) - f_c$. This in turn suggests that both pass-band droop and selectivity of GCF filters are preserved by the approximations of the multipliers.

An important question is still open. We still need to quantify the extent of the effects of the coefficient approximations on the frequency response $\widetilde{H}_{\mathrm{GCF}_3}(z)$. In brief, the basic question we want to answer is as follows. What are the approximation errors $\Delta r_u, \forall u = p_p + 1, \ldots, \underset{\sim}{p} - 1$, and $\Delta h_P(n), \forall n \in [0, 3D_1 - 3]$, that we can tolerate on $\widetilde{H}_{\mathrm{GCF}_3}(z)$? The answer to this question is the focus of the next section. It is anticipated that whatever the condition on the maximum approximation error tolerated on the frequency response $\widetilde{H}_{\mathrm{GCF}_3}(e^{j\omega})$, it should be related to the behavior of such a function around the folding bands, since both pass-band droop and selectivity of these filters are mainly unaffected by the approximation of the multipliers.

V. Estimation of Zero Displacements Due to Coefficient Approximations

Besides improving the selectivity on the frequency $(1/D) - f_c$, GCF filters provide improved $\Sigma\Delta$ QN rejection around the folding bands with respect to classical, equal-order comb filters [9]. However, coefficient approximations can have detrimental effects on the zero locations in the z-plane, and, accordingly, can worsen $\Sigma\Delta$ QN rejection performance around the folding bands. Therefore, it is useful to estimate the effects of coefficient approximations on the actual $\Sigma\Delta$ QN rejection performance guaranteed by filter $\widetilde{H}_{\mathrm{GCF}_3}(e^{j\omega})$ by estimating the induced zero displacements. Next three sections address this topic by first examining filters $H_P(z)$ and $H_N(z)$ separately[4], and then deducing some hints from the derived theoretical analysis.

A. Displacements of Zeros Belonging to $H_P(z)$

In this section, the focus is on the evaluation of the errors Δz_k on the locations of the zeros of $H_P(z)$ due to the approximations of the coefficients $h_P(n)$ in the polyphase filter $H_P(e^{j\omega})$. First of all, notice that $H_P(z)$ places its $3 \cdot D_1 - 3$ zeros in the following z locations:

$$z_k = \begin{cases} e^{+j2\pi\frac{k}{D_1}}, & \forall k = 1, \ldots, \left\lfloor \frac{D_1}{2} \right\rfloor \\ e^{-j2\pi\frac{k}{D_1}}, & \forall k = 1, \ldots, \left\lfloor \frac{D_1}{2} \right\rfloor - 1 \\ e^{+j2\pi\left(\frac{k}{D_1} + q f_c\right)}, & \forall k = 1, \ldots, \left\lfloor \frac{D_1}{2} \right\rfloor - 1 \\ e^{-j2\pi\left(\frac{k}{D_1} + q f_c\right)}, & \forall k = 1, \ldots, \left\lfloor \frac{D_1}{2} \right\rfloor - 1 \\ e^{\pm j2\pi\left(\frac{k}{D_1} - q f_c\right)}, & \forall k = 1, \ldots, \left\lfloor \frac{D_1}{2} \right\rfloor. \end{cases}$$

The z-transfer function $H_P(z)$ in (13) can be expressed in a form emphasizing its zeros

$$H_P(z) = \prod_{k=1}^{L-1} (1 - z_k z^{-1}) \tag{29}$$

[4]This is possible by virtue of the sensitivity analysis derived above: zeros of both $H_P(z)$ and $H_N(z)$ affect different folding bands. In other words, each pair of conjugate complex zeros affects the behavior of the frequency response in only one folding band.

whereby $L = 3 \cdot D_1 - 2$. Due to the approximation of the coefficients $h_P(n)$, the set of zeros becomes $\{\widetilde{z}_k = z_k + \Delta z_k, \forall k = 1, \ldots, L-1\}$

$$\widetilde{H}_P(z) = \prod_{k=1}^{L-1} (1 - \widetilde{z}_k z^{-1}).$$

Zero displacements Δz_k can be related to the coefficient approximations Δh_P as follows:

$$\Delta z_i = \sum_{\eta=1}^{L} \frac{\partial z_i}{\partial h_P(\eta)} \Delta h_P(\eta) \tag{30}$$

since there are L coefficients $h_P(n)$ with $n \in [0, L-1]$.

Upon noting that

$$\frac{\partial H_P(z)}{\partial h_P(\eta)}_{|_{z=z_i}} = \frac{\partial H_P(z)}{\partial z}_{|_{z=z_i}} \cdot \frac{\partial z_i}{\partial h_P(\eta)}$$

it is straightforward to obtain

$$\frac{\partial H_P(z)}{\partial h_P(\eta)}_{|_{z=z_i}} = -z^{-\eta}_{|_{z=z_i}} = -z_i^{-\eta}$$

by employing (13), and

$$\frac{\partial H_P(z)}{\partial z}_{|_{z=z_i}} = \left\{ \sum_{k=1}^{L-1} \frac{z_k}{z^2} \prod_{l=1, l\neq k}^{L-1} (1 - z_l z^{-1}) \right\}_{|_{z=z_i}}$$

by deriving (29) with respect to z. Finally, after some algebra (30) can be rewritten as follows:

$$\Delta z_i = -\sum_{\eta=1}^{L} \frac{z_i^{-\eta} \Delta h_P(\eta)}{\left\{ \sum_{k=1}^{L-1} \frac{z_k}{z^2} \prod_{l=1, l\neq k}^{L-1} (1 - z_l z^{-1}) \right\}_{|_{z=z_i}}} \tag{31}$$

which is the displacement of the ith zero z_i due to the approximations of all coefficients $h_P(n)$ belonging to the polyphase filter decimating by D_1.

Fig. 8 shows the maximum Δz_i over all the set of zeros indexed by $i = 1, \ldots, L$, as a function of the approximation error $\Delta h_P(\eta) = \Delta h_P$, assumed to be the same for all coefficients, for various values of D_1, $D_2 = 4$, and $\nu = 4$. Curves shown in the figure can be considered as the worst case zero displacement due to the approximations of coefficients $h_P(n)$.

B. Displacements of Zeros Belonging to $H_N(z)$

In this section, the focus is on the evaluation of the displacements Δz_k of the zeros in $H_N(z)$ due to the approximation of the coefficients r_u belonging to $H_N(z)$. Error Δz_i on the ith

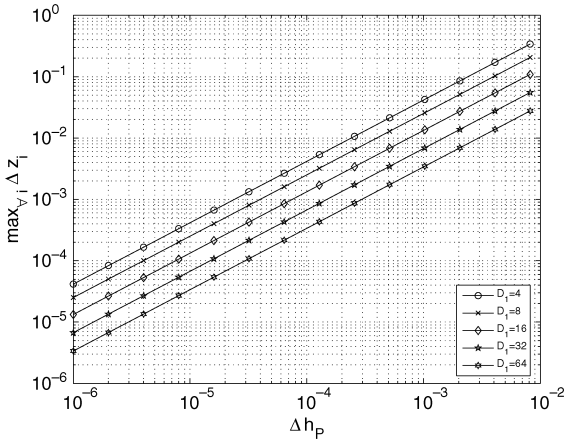

Fig. 8. Maximum zero displacement over all the set of coefficients $h_P(n)$ as a function of the approximation error Δh_P. The results assume the same error Δh_P for all the coefficients $h_P(n)$. Parameters are as follows: $D_2 = 4$, and $\nu = 4$.

zero can be related to the approximation errors of multipliers r_u as follows:

$$\Delta z_i = \sum_{u=p_p+1}^{p-1} \frac{\partial z_i}{\partial r_u} \Delta r_u. \tag{32}$$

Upon noting that

$$\frac{\partial H_N(z)}{\partial r_u}_{|_{z=z_i}} = \frac{\partial H_N(z)}{\partial z}_{|_{z=z_i}} \cdot \frac{\partial z_i}{\partial r_u}$$

after some algebra on (10), it is possible to obtain

$$\frac{\partial H_N(z)}{\partial r_u}_{|_{z=z_i}} = \left\{ \left(z^{-2^u} + z^{-2\cdot 2^u} \right) \times \prod_{k=p_p+1, k\neq u}^{p-1} \left[1 + r_k \left(z^{-2^k} + z^{-2\cdot 2^k} \right) + z^{-3\cdot 2^k} \right] \right\}_{|_{z=z_i}}. \tag{33}$$

By deriving (10) with respect to z, it is possible to write

$$\begin{aligned} \frac{\partial H_N(z)}{\partial z}_{|_{z=z_i}} = \sum_{k=p_p+1}^{p-1} \Big\{ \Big[& r_k \left(2^k z^{-2^k-1} - 2 \cdot 2^k z^{-2\cdot 2^k-1} \right) \\ & -3 \cdot 2^k z^{-3\cdot 2^k} \Big] \\ & \cdot \prod_{l=p_p+1, l\neq k}^{p-1} \Big[1 + r_l \left(z^{-2^l} + z^{-2\cdot 2^l} \right) \\ & + z^{-3\cdot 2^l} \Big] \Big\}_{|_{z=z_i}}. \end{aligned} \tag{34}$$

Finally, (32) can be evaluated by substituting the ratio between (33) and (34) in place of $\partial z_i / \partial r_u$.

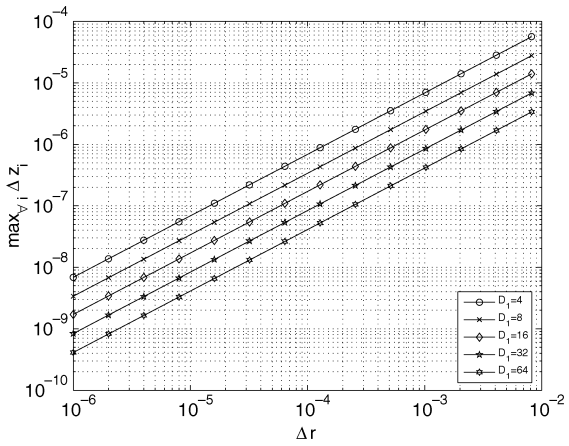

Fig. 9. Maximum zero displacement over all the set of coefficients r_u as a function of the approximation error Δr. Curves assume the same error Δr for all the multipliers r_u. Parameters are as follows: $D_2 = 4$, and $\nu = 4$.

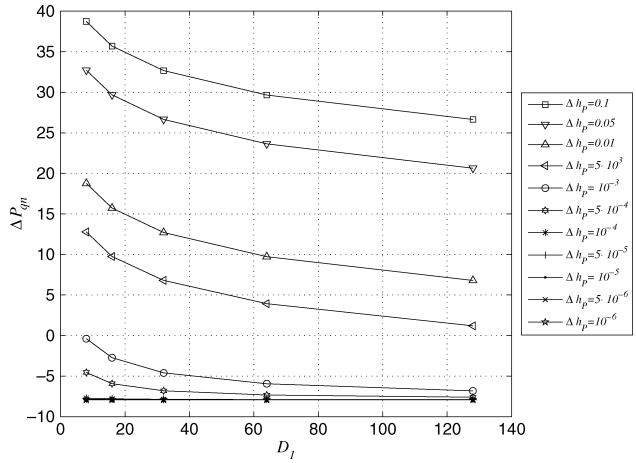

Fig. 10. behavior of the difference $\Delta P_{qn} = \widetilde{P}_{qn|\mathrm{dB}} - P_{qn|\mathrm{dB}}$ as a function of the decimation factor D_1 and for various values of the approximation errors Δh_P shown in the legend.

Fig. 9 shows the maximum Δz_i over all the set of zeros belonging to $H_N(z)$, as a function of the approximation error $\Delta r_u = \Delta r$, assumed to be the same for all multipliers, for various values of D_1, $D_2 = 4$ and $\nu = 4$.

A quick comparison between the results shown in Figs. 8 and 9 reveals that the maximum zero displacement of the zeros belonging to $H_N(z)$ is much smaller than the one experienced by zeros belonging to $H_P(n)$. There are at least two basic reasons for such a behavior. First, the number of multipliers r_u is very small with respect to the number of coefficients $h_P(n)$ of the polyphase section. Secondly, any error Δr_u slightly rotates the zeros belonging to the uth decimation cell in $H_N(z)$ leaving them on the unit circle. This follows from the z-transfer function $[1+r_u(z^{-1}+z^{-2})+z^{-3}]$ of the uth decimation stage. On the other hand, approximation errors $\Delta h_P(n)$ can also move the zeros of $H_P(z)$ outside the unit circle in the z-plane worsening the $\Sigma\Delta$ QN rejection performance of the decimation filter.

The previous analysis suggests that the most critical filter in the partial polyphase architecture is the polyphase section $H_P(e^{j\omega})$. In order to deduce the maximum tolerable approximation error over the set of coefficients $\Delta h_P(n)$, the behavior of filter $H_P(e^{j\omega})$ around the folding bands should be further investigated. This is the topic addressed in the next section.

C. Design Considerations

The $\Sigma\Delta$ QN power falling inside the folding bands $[(k/D_1)-f_c, (k/D_1)+f_c]$, $\forall k = 1, \ldots, \lfloor D_1/2 \rfloor$, can be defined[5] as [1]

$$P_{qn} = \sum_{k=1}^{\lfloor \frac{D_1}{2} \rfloor} \int_{\frac{k}{D_1}-f_c}^{\frac{k}{D_1}+f_c} \left| H_P(e^{j\omega}) \right|^2 S_B(f_d) df_d \qquad (35)$$

where $S_B(f_d)$, the power spectral density of the $\Sigma\Delta$ QN, can be expressed as $S_B(f_d) = S_e(f_d) \cdot [2\sin(\pi f_d)]^{2B}$. In the previous relation $S_e(f_d) = \Delta^2/12 f_s$ is the power spectral density of the sampled noise under the hypothesis of representing the QN as a white noise [1], Δ is the quantization level of the quantizer contained in the $\Sigma\Delta$ modulator [1], and f_s is the $\Sigma\Delta$ sampling rate.

In order to quantify the $\Sigma\Delta$ QN rejection performance of filter $\widetilde{H}_P(z)$ embedding the approximated multipliers $\widetilde{h}_P(n) = h_P(n) + \Delta h_P(n)$, with respect to a classical third-order comb filter, the following performance metric, ΔP_{qn}, can be evaluated

$$\Delta P_{qn} = \frac{\sum_{k=1}^{\lfloor \frac{D_1}{2} \rfloor} \int_{\frac{k}{D}-f_c}^{\frac{k}{D}+f_c} \left| \widetilde{H}_P(f_d) \right|^2 S_B(f_d) df_d}{\sum_{k=1}^{\lfloor \frac{D_1}{2} \rfloor} \int_{\frac{k}{D}-f_c}^{\frac{k}{D}+f_c} \left| H_{C_3}(f_d) \right|^2 S_B(f_d) df_d}. \qquad (36)$$

The behavior of ΔP_{qn}-[dB] as a function of D_1 is shown in Fig. 10, for various values of Δh_P, i.e., the approximation error which is assumed to be the same for all the coefficients $h_P(n)$. It is worth noticing that negative values of ΔP_{qn}-[dB] mean that the designed filter guarantees improved $\Sigma\Delta$ QN rejection performance with respect to a classical third-order comb filter. Results in Fig. 10 show that $\Sigma\Delta$ QN rejection improvements can still be achieved upon approximating each coefficient $h_P(n)$ within an error less or equal to 10^{-3}.

This in turn suggests that it is possible to optimize each multiplier $h_P(n)$ in the polyphase filter $H_P(z)$ by resorting to power-of-2 (PO2) approximation of the coefficients within an approximation error as low as 10^{-3}, without affecting the $\Sigma\Delta$ QN rejection performance of the polyphase filter around the folding bands for any $D_1 \geq 32$.

Fig. 11 shows the behaviors of both the frequency response of filter $H^*_{\mathrm{GCF}_3}(e^{j\omega})$ employing approximated coefficients $\widetilde{h}_P(n) = h_P(n) + \Delta h_P(n)$, and the frequency response of filter $H_{\mathrm{GCF}_3}(e^{j\omega})$ embedding the real coefficients $h_P(n)$, for $D = D_1 = 64$, $\nu = 4$, and $\Delta h_P(n) = \Delta h_P = 10^{-3}$, $\forall n$. This is the most critical case in which a full polyphase architecture is employed. The lower subplot shows the local behavior of both frequency responses around some folding bands. Notice that both curves are superimposed, even though $H^*_{\mathrm{GCF}_3}(e^{j\omega})$ employs coefficients approximated with an error equal to 10^{-3}. The approximation of the multipliers $h_P(n)$ with PO2 coefficients is beyond the scope of this work. Nevertheless, many excellent works have been proposed in literature for

[5]Note that (35) is valid only if the noise transfer function (NTF) of the modulator is maximally flat, i.e., it does not contain stabilizing poles. In higher order modulators this requires multibit feedback structures.

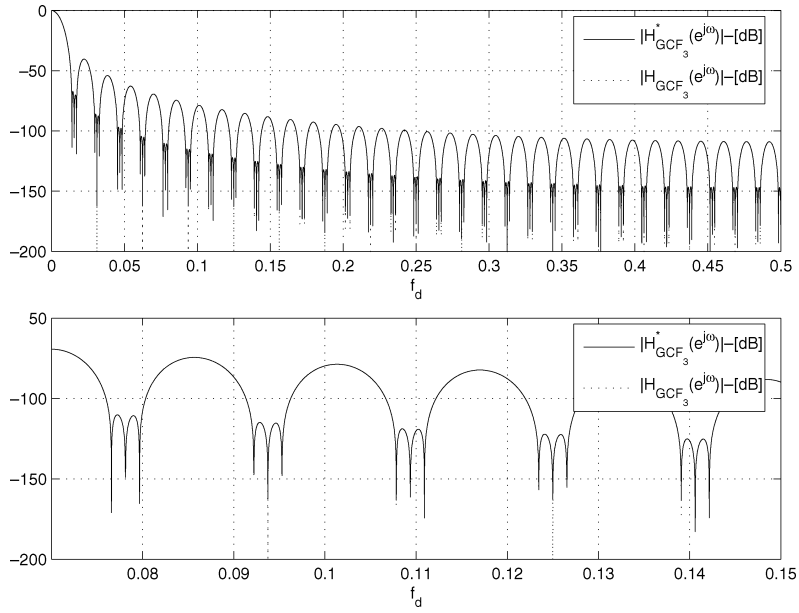

Fig. 11. Modulo of the frequency response of filter $H^{*}_{\mathrm{GCF}_3}(e^{j\omega})$ employing approximated coefficients $\widetilde{h}_P(n) = h_P(n) + \Delta h_P(n)$ (continuous curve), and frequency response of filter $H_{\mathrm{GCF}_3}(e^{j\omega})$ embedding the real coefficients $h_P(n)$, for $D = D_1 = 64$, $\nu = 4$, and $\Delta h_P(n) = \Delta h_P = 10^{-3}$, $\forall n$. Lower subplot shows the behaviors of such functions around five folding bands.

obtaining the best PO2 coefficient approximation within a predefined error. We invite the interested readers to refer to papers [18]–[20].

Let us summarize the main design hints deduced from the proposed sensitivity analysis of partial polyphase GCF filters. A summary of the key design parameters is shown in Table III.

- Both pass-band droop and selectivity performance of GCF filters are mainly unaffected by the approximation of the multipliers embedded in the decimation filter. Practically speaking, this means that such performance are the one already deduced in the companion paper [9].
- Upon approximating each multiplier of the polyphase section with an approximation error less or equal to 10^{-3}, it is possible to preserve the $\Sigma\Delta$ QN rejection performance of GCF filters with respect to classical, equal-order comb filters, for a wide range of decimation factors D_1 as noted in the abscissa of Fig. 10.

TABLE III
SET OF THE KEY DESIGN PARAMETERS

$D = D_1 \cdot D_2 = 2^p$
Dec. factor of $H_{GCF_3}(e^{j\omega}) = H_P(e^{j\omega})H_N(e^{j\omega})$
$D_1 = 2^{p_p+1}$
Dec. factor of $H_P(e^{j\omega})$, the polyphase subfilter
Imp. response $h_P(n)$ (see (11)) has length $L = 3D_1 - 2$
$D_2 = 2^{p-p_p-1}$
Dec. factor of $H_N(e^{j\omega})$. Integer $p - p_p - 1$ is the number of non recursive filters decimating by 2 in Fig. 3
$p_p \in \{-1, \ldots, p-1\}$,
• Full Cascaded Architecture
If $p_p = -1 \Rightarrow D_1 = 1,\ D_2 = 2^p \Rightarrow H_{GCF_3}(z) = H_N(z)$,
$H_{GCF_3}(z) = \prod_{i=0}^{p-1}\left[1 + r_i \cdot \left(z^{-2^i} + z^{-2\cdot 2^i}\right) + z^{-3\cdot 2^i}\right]$
$r_i = 1 + 2\cos\left(2^i\alpha\right),\ \forall i = 0, \ldots, p-1$
• Full Polyphase Architecture
If $p_p = p - 1 \Rightarrow D_1 = 2^p,\ D_2 = 1$
$\Rightarrow H_{GCF_3}(z) = H_P(z)$ in (13)
• Partial Polyphase Architecture
If $p_p \in \{0, \ldots, p-2\} \Rightarrow H_{GCF_3}(z) = H_P(z)H_N(z)$
ν, Dec. factor of the filter $H_2(z)$ in the cascade architecture shown in Fig. 1
$\rho = D \cdot \nu = D_1 \cdot D_2 \cdot \nu$, oversampling factor
$\alpha = 2\pi\lvert q\rvert f_c$, opt. zero rotations around the folding bands
$f_c = \frac{1}{2\rho}$, bandwidth of the signal $x(nT_s)$ at the output of the $\Sigma\Delta$ modulator in Fig. 1

D. Computational Complexity and Comparisons

In this section we define the computational complexity of the proposed architecture and present some comparisons with other techniques proposed in literature.

The computational complexity of the proposed decimation architecture can be readily evaluated upon discussing the general scheme noted in Fig. 3. Given an appropriate split of the overall decimation factor D, i.e., $D = D_1 \cdot D_2$, the partial polyphase architecture $H_{\mathrm{GCF}_3}(z) = H_P(z)H_N(z)$ presents a computational complexity which can be roughly evaluated in terms of the number of its multipliers as follows.

The filter cell $H_P(z)$ employs $3D_1 - 2$ multipliers belonging to the polyphase components $E_k(z)$, $\forall k = 0, \ldots, D_1 - 1$. Such multipliers operate at the reduced rate f_s/D_1, whereby f_s is the sampling frequency of the incoming data.

The filter cell $H_N(z)$ presents a multiplier operating at the very reduced rate $f_s/(D_1 \cdot 2^i)$ for any stage $i \in \{0, \ldots, p - p_p - 2\}$. The complexity of the PPoly filter $H_{\mathrm{GCF}_3}(z)$ is summarized in the first row in Table IV. Since the proposed architecture is non recursive, multipliers belonging to $H_P(z)$ and $H_N(z)$ can be approximated as PO2 coefficients by following the guidelines given in the previous sections, without any instability problem. By following this design approach, the implementation of PPoly filters does not require any real multiplier. Notice that PO2 coefficients cannot be employed with a recursive architecture: the reason relies in the fact that, in general, a recursive architecture

TABLE IV
COMPARISONS AMONG DECIMATION FILTERS

Filter Class	No. of Multipliers	Sample Rate
PPoly	$3D_1 - 2$ $i \in \{0, \ldots, p - p_p - 2\}$	f_s/D_1 $f_s/(D_1 \cdot 2^i)$
MSDF [6]	1 1	f_s f_s/D
SMCF [16], $H_{11}(z)$	1 3	f_s f_s/D
SMCF [16], $H_{12}(z)$	1 4	f_s f_s/D

introduces some poles that, after quantization, do not get cancelled by the appropriate zeros.

Among the decimation filters recently proposed in literature, the class of modified-sinc decimation filters (MSDFs) proposed in [6], and the class of sharpened modified comb filters (SMCFs) proposed in [16] are, perhaps, the ones somewhat related to the decimation filters investigated in this work. Briefly, such classes were proposed in the attempt to design decimation filters with improved QN rejection as well as reduced pass-band droop penalties with respect to classical comb filters.

The third-order recursive architecture of MSDFs proposed in [6], features a multiplier operating at the data sample rate, f_s, as well as a multiplier operating at the decimated rate f_s/D, as summarized in the second row in Table IV. In general, higher order MSDF filters require an increasing number of multipliers [16].

The last comparison regards the technique proposed in [16] for the design of SMCF filters. Based on the transfer function of SMCF filters, the computational complexities of the first low-order filters $H_{11}(z)$ and $H_{12}(z)$ are summarized in the two last rows in Table IV. Notice that filters $H_{11}(z)$ and $H_{12}(z)$ present an increased number of multipliers operating at the decimated sample rate f_s/D with respect to MSDFs of equal order. This is the price to be paid for reducing the pass-band droop penalty of MSDFs, while guaranteeing improved QN rejection performance around the folding bands with respect to classical comb filters.

VI. CONCLUSION

This paper focused on the design of GCFs by proposing a novel partial polyphase architecture with the aim to reduce the data rate after the $\Sigma\Delta$ A/D conversion. We proposed a mathematical framework in order to analyze both the sensitivity of the frequency response and the displacements of the zeros in the filter transfer functions due to the approximation of the multipliers embedded in the proposed filters.

We also derived the impulse response of a third-order sample GCF filter that we used as a reference scheme throughout the paper.

APPENDIX

In this Appendix, we derive the impulse response $h_{\mathrm{GCF}_3}(n)$, $\forall n = 0, \ldots, 3D - 3$, of a third-order GCF filter decimating by D. The proof relies on repeated applications of the inverse z-transform on the product of two analytical functions $X_1(z)$ and $X_2(z)$ related to two discrete-time sequences, $x_1(n)$ and $x_2(n)$

$$Z^{-1}\left[X_1(z)X_2(z)\right] = x_1(n) \star x_2(n) = \sum_{k=-\infty}^{+\infty} x_1(k)x_2(n-k). \quad (37)$$

First of all, consider the transfer function in (5), and define as $X_t(z)$ the numerator z-polynomial

$$X_t(z) = (1 - z^{-D}e^{j\alpha D})(1 - z^{-D}e^{-j\alpha D})(1 - z^{-D}) = [1 - rz^{-D} + rz^{-2D} - z^{-3D}]$$

whereby $r = 1 + 2\cos(\alpha D)$. The discrete-time, causal sequence with z-transfer function $X_t(z)$ can be written as follows:

$$x_t(n) = \delta(n) - r\delta(n - D) + r\delta(n - 2D) - \delta(n - 3D) \quad (38)$$

whereby $\delta(n)$ is the discrete-time unit impulse centered in $n = 0$.

Let us define the following pairs of transfer functions along with the respective discrete-time sequences [17]

$$Y_1(z) = \frac{1}{1 - z^{-1}} \quad \longleftrightarrow \quad y_1(n) = u(n)$$
$$Y_2(z) = \frac{1}{1 - z^{-1}e^{-j\alpha}} \quad \longleftrightarrow \quad y_2(n) = e^{-j\alpha}u(n)$$
$$Y_3(z) = \frac{1}{1 - z^{-1}e^{j\alpha}} \quad \longleftrightarrow \quad y_3(n) = e^{+j\alpha}u(n)$$

whereby $u(n)$ is the discrete-time unitary-step sequence.

With the setup above, $H_{\mathrm{GCF}_3}(z)$ in (5) can be rewritten as follows:

$$H_{\mathrm{GCF}_3}(z) = X_t(z) \cdot Y_1(z) \cdot Y_2(z) \cdot Y_3(z).$$

Upon applying (37) to the z-function $W_1(z) = X_t(z)Y_1(z)$, it is possible to obtain

$$w_1(n) = \sum_{k_1=-\infty}^{+\infty} x_t(k_1)y_1(n - k_1). \quad (39)$$

Applying (37) to the z-function $W_2(z) = W_1(z)Y_2(z)$, and employing (39), it is possible to obtain

$$w_2(n) = \sum_{k_2=-\infty}^{+\infty} w_1(k_2)y_2(n-k_2) = \sum_{k_2=-\infty}^{+\infty}\sum_{k_1=-\infty}^{+\infty} x_t(k_1)y_1(k_2-k_1)y_2(n-k_2). \quad (40)$$

Finally, applying (37) to the z-function $H_{\mathrm{GCF}_3}(z) = W_3(z) = W_2(z)Y_3(z)$, and employing (40), it is possible to obtain

$$h_{\mathrm{GCF}_3}(n) = \sum_{k_3=-\infty}^{+\infty} w_2(k_3)y_3(n - k_3) = \sum_{k_3=-\infty}^{+\infty}\sum_{k_2=-\infty}^{+\infty}\sum_{k_1=-\infty}^{+\infty} [x_t(k_1)y_1(k_2 - k_1) \cdot y_2(k_3-k_2)y_3(n-k_3)]. \quad (41)$$

Upon substituting the respective expressions of the sequences $y_i(n), \forall i = 1, \ldots, 3$ in (39), it is possible to write

$$h_{\mathrm{GCF}_3}(n) = \sum_{k_3=-\infty}^{+\infty} \sum_{k_2=-\infty}^{+\infty} \sum_{k_1=-\infty}^{+\infty} [x_t(k_1)u(k_2-k_1) \cdot e^{-j\alpha(k_3-k_2)}u(k_3-k_2)e^{+j\alpha(n-k_3)}u(n-k_3)] \quad (42)$$

By exploiting the definitions of the unitary-step sequences, it is possible to observe the following relations:

$$u(k_2-k_1) = \begin{cases} 1 & \forall k_2 \geq k_1 \\ 0 & \forall k_2 < k_1 \end{cases}$$
$$u(k_3-k_2) = \begin{cases} 1 & \forall k_3 \geq k_2 \\ 0 & \forall k_3 < k_2 \end{cases}$$
$$u(n-k_3) = \begin{cases} 1 & \forall n \geq k_3 \\ 0 & \forall n < k_3. \end{cases}$$

Based on these observations, we can reduce the upper limits of the summations in (42) as follows:

$$h_{\mathrm{GCF}_3}(n) = \sum_{k_3=-\infty}^{n} \sum_{k_2=-\infty}^{k_3} \sum_{k_1=-\infty}^{k_2} [x_t(k_1) \cdot e^{-j\alpha(k_3-k_2)}e^{+j\alpha(n-k_3)}]. \quad (43)$$

By observing that the sequence $x_t(k_1)$ is causal (see (38)), i.e., $x_t(k_1) = 0, \forall k_1 < 0$, it is possible to obtain

$$h_{\mathrm{GCF}_3}(n) = e^{+j\alpha n} \sum_{k_3=0}^{n} e^{-2j\alpha k_3} \sum_{k_2=0}^{k_3} e^{j\alpha k_2} \sum_{k_1=0}^{k_2} x_t(k_1). \quad (44)$$

Notice that the impulse response $h_{\mathrm{GCF}_3}(n)$ generalizes the one of the classical third-order comb decimation filter, and, it is composed by $3D-2$ coefficients over the time interval ranging from 0 to $3D-3$. Equ. (44) can also be used as an on-line algorithm for generating the coefficients of the GCF impulse response $h_{\mathrm{GCF}_3}(n)$ by simply solving the three nested summations for each $n = 0, \ldots, 3D-3$.

As a note aside, notice that by imposing $\alpha = 0$ in (44), it is possible to obtain the impulse response of a classical third-order comb filter.

REFERENCES

[1] S. R. Norsworthy, R. Schreier, and G. C. Temes, *Delta-Sigma Data Converters, Theory, Design, and Simulation*. New York: IEEE Press, 1997.

[2] E. B. Hogenauer, "An economical class of digital filters for decimation and interpolation," *IEEE Trans. Acoust., Speech, Signal Process.*, vol. ASSP-29, no. 2, pp. 155–162, Apr. 1981.

[3] J. C. Candy, "Decimation for sigma delta modulation," *IEEE Trans. Comm.*, vol. COM-34, no. 1, pp. 72–76, Jan. 1986.

[4] R. E. Crochiere and L. R. Rabiner, *Multirate Digital Signal Processing*. Upper Saddle River, NJ: Prentice-Hall PTR, 1983.

[5] S. Chu and C. S. Burrus, "Multirate filter designs using comb filters," *IEEE Trans. Circuits Syst.*, vol. CAS-31, no. 11, pp. 913–924, Nov. 1984.

[6] L. Lo Presti, "Efficient modified-sinc filters for sigma-delta A/D converters," *IEEE Trans. Circuits Syst. II, Anlog Digit. Signal Process.*, vol. 47, no. 11, pp. 1204–1213, Nov. 2000.

[7] M. Laddomada, L. Lo Presti, M. Mondin, and C. Ricchiuto, "An efficient decimation sinc-filter design for software radio applications," in *Proc. IEEE SPAWC*, Mar. 20–23, 2001, pp. 337–339.

[8] L. Lo Presti and A. Akhdar, "Efficient antialising decimation filter for $\Sigma\Delta$ converters," in *Proc. ICECS98*, Sep. 1998, vol. 1, pp. 367–370.

[9] M. Laddomada, "Generalized comb decimation filters for $\Sigma\Delta$ A/D converters: Analysis and design," *IEEE Trans. Circuits Syst. I, Reg. Papers*, vol. 54, no. 5, pp. 994–1005, May 2007.

[10] Y. Gao, J. Tenhunen, and H. Tenhunen, "A fifth-order comb decimation filter for multi-standard transceiver applications," in *Proc. IEEE ISCAS 2000*, May 2000, pp. III-89–III-92.

[11] H. Aboushady, Y. Dumonteix, M. Louërat, and H. Mehrez, "Efficient polyphase decomposition of comb decimation filters in $\Sigma\Delta$ analog-to-digital converters," *IEEE Trans. Circuits Syst. II, Analog Digit. Signal Process.*, vol. 48, no. 10, pp. 898–903, Oct. 2001.

[12] A. Y. Kwentus, Z. Jiang, and A. N. Willson, Jr., "Application of filter sharpening to cascaded integrator-comb decimation filters," *IEEE Trans. Signal Process.*, vol. 45, no. 2, pp. 457–467, Feb. 1997.

[13] G. Jovanovic-Dolecek and S. K. Mitra, "A new two-stage sharpened comb decimator," *IEEE IEEE Trans. Circuits Syst. I, Reg. Papers*, vol. 52, no. 7, pp. 1414–1420, Jul. 2005.

[14] M. Laddomada and M. Mondin, "Decimation schemes for $\Sigma\Delta$ A/D converters based on Kaiser and Hamming sharpened filters," *Proc. IEE Vision, Image, Signal Process.*, vol. 151, no. 4, pp. 287–296, Aug. 2004.

[15] F. Daneshgaran and M. Laddomada, "A novel class of decimation filters for $\Sigma\Delta$ A/D converters," *Wireless Commun. Mobile Comput.*, vol. 2, no. 8, pp. 867–882, Dec. 2002.

[16] M. Laddomada, "Comb-based decimation filters for $\Sigma\Delta$ A/D converters: Novel schemes and comparisons," *IEEE Trans. Signal Process.*, vol. 55, no. 5, pt. 1, pp. 1769–1779, May 2007.

[17] A. Antoniou, *Digital Signal Processing: Signals, Systems, and Filters*. New York: McGraw-Hill, 2005, 0-07-145425-X.

[18] Y. C. Lim and S. R. Parker, "FIR filter design over a discrete powers-of-two coefficient space," *IEEE Trans. Acoust., Speech, Signal Process.*, vol. ASSP-31, no. 3, pp. 583–591, Jun. 1983.

[19] W. J. Oh and Y. H. Lee, "Implementation of programmable multiplierless FIR filters with powers-of-two coefficients," *IEEE Trans. Circuits Syst. II, Analog Digit. Signal Process.*, vol. 42, no. 8, pp. 553–556, Aug. 1995.

[20] D. Li, Y. C. Lim, Y. Lian, and J. Song, "A polynomial-time algorithm for designing FIR filters with powers-of-two coefficients," *IEEE Trans. Signal Process.*, vol. 50, no. 8, pp. 1935–1941, Aug. 2002.

Massimiliano Laddomada (S'00–M'03) was born in 1973. He received the degree in electronics engineering and the Ph.D. degree in communications engineering from Politecnico di Torino, Turin, Italy, in 1999 and 2003, respectively.

From June 2000 to March 2001, he was a Visiting Researcher at California State University (CSU), and a Consultant Engineer with Technoconcepts, Inc., Los Angeles, a start-up company specializing in Software Radio. He was a Research Associate with Politecnico di Torino from 2004 to 2008, and he has been a part-time faculty as CSU since 2006. In 2008, he joined the Electrical Engineering Department, Texas A&M University, Texarkana, as an Assistant Professor. His research is mainly in digital signal processing and wireless communications, especially modulation and coding, including turbo codes and, more recently, networks coding.

Dr. Laddomada was awarded a five-year open-ended fellowship by E.D.S.U. in recognition of his university career as an Electronics Engineer. In 2003, he was awarded with the *Premio Zucca per l'Innovazione nell'ICT* from Unione Industriale of Turin. Currently, he is serving as a member of the editorial boards of IEEE COMMUNICATIONS SURVEYS AND TUTORIALS, and the *International Journal of Digital Multimedia Broadcasting* (Hindawi).